Electronic states in Si nanocrystal thin films

Rong Zhang,[1,a)] Hua Wu,[2] Xinyi Chen,[3] and Wenzhong Shen[3,b)]
[1]*Department of Physics, Shanghai Maritime University, 1550 Pudong Avenue, Shanghai 200135, People's Republic of China*
[2]*Department of Applied Physics, Dong Hua University, 2999 Ren Min Road, Shanghai 201620, People's Republic of China*
[3]*Department of Physics, Laboratory of Condensed Matter Spectroscopy and Opto-Electronic Physics, Shanghai Jiao Tong University, 1954 Hua Shan Road, Shanghai 200030, People's Republic of China*

(Received 9 April 2009; accepted 22 May 2009; published online 18 June 2009)

We report on the investigation of electronic states in hydrogenated nanocrystalline silicon (nc-Si:H) thin films through the electronic transitions by photocurrent measurements. Higher photocurrent response has been observed above the bulk Si band gap of 1.05 eV in the nc-Si:H films with larger crystalline faction. We attribute the high photocurrent response to the enhancement of the photocarrier transport due to the formation of the extended electronic states and the direct electronic transition caused by the discrete states. The interaction of the extended states and discrete states has been further demonstrated by the Fano resonance observed in the Raman scattering spectra. © *2009 American Institute of Physics*. [DOI: 10.1063/1.3154520]

Hydrogenated nanocrystalline silicon (nc-Si:H) thin films have attracted considerable interest due to their applications on the promising silicon solar energy photovoltaic industry with the market demand of green energy greatly increasing in recent years.[1] There are a few merits of photovoltaic and photocurrent response in the nc-Si:H thin films. The main advantage of the nc-Si:H thin film is the low cost due to its growth temperature below 300 °C realized by the plasma-enhanced chemical vapor deposition (PECVD) in the region adjacent to the phase transition from amorphous to crystalline state. Furthermore, the transition material of the nc-Si:H thin film for photovoltaic and photocurrent response is a compromise between a crystalline material and amorphous material.[2] The nc-Si:H thin film is a possible way to take advantage of a relatively high conductivity and a relatively high optical absorption due to its double features of ordered and disordered structure.

Recently, we have realized a series of high-quality nc-Si:H thin films (where Si nanocrystals are uniformly embedded in *a*-Si:H networks) with different average grain sizes and crystalline fractions by tuning the growth conditions of the PECVD system. Moreover, the conductivity of the nc-Si:H films can be tuned varying from the order of 10^{-4} to the order of 10^{2} S cm^{-1}.[3] This allows us to investigate the variation of the electronic state of the nc-Si:H thin films caused by the change of structure order. The study of the electronic states in the transition material of the nc-Si:H thin film is quite few up to now. However, it is very important to understand how to improve the photovoltaic generation efficiency by the nc-Si:H thin films.

In order to obtain a whole physical picture of electronic states variations detected by photocurrent response, we prepared the *a*-Si:H thin film, nc-Si:H thin film, and c-Si samples with the crystalline fraction nearly varying in the full range of 0%–100%. First, we used the p^+ c-Si substrate to form superior Schottky-barrier structure for the *a*-Si:H or nc-Si:H thin films with very low crystalline fraction (i.e., samples E and D), so as to improve the photocarrier collection efficiency by the internal depletion region of the heterostructure.[4] Second, the electronic transport was improved to be high enough within high crystalline fraction nc-Si:H thin film, which could allow us to directly collect photocarriers in the nc-Si:H thin film grown on glass (as in sample C) without the aid of heterostructure. Third, *p*-type c-Si was used as substrate again to grow the nc-Si:H thin film with structural order further improved as in sample B.[3] Finally, one typical c-Si *n-p* junction sample A was used as a perfect structural ordered sample for reference.

The nc-Si:H thin film samples were prepared in a rf (13.56 MHz and power density of 0.3–0.5 W/cm^2) capacitive-coupled PECVD system from silane (SiH_4) and hydrogen (H_2) doped with phosphine (PH_3).[5,6] We deposited the studied samples with the percentage content of silane (SiH_4/SiH_4+H_2) 1% and phosphine (PH_3/SiH_4) 0.8% at 250 °C under the chamber pressure of 0.4–1.0 Torr. The undoped *a*-Si:H thin film sample is also grown in the PECVD system on the p^+ c-Si substrate under very low pressure of 0.2 Torr and low power density of 0.02 W/cm^2 with the percentage content of silane (SiH_4/SiH_4+Ar) 20% and takes on *n*-type conduction. The nc-Si:H thin film samples, together with the *a*-Si:H sample E and the c-Si sample A as references, have been used for the study and corresponding sample information of growth conditions and configurations are listed in Table I. The photocurrent measurements were carried out on a Nicolet Nexus 870 Fourier transform infrared spectrometer calibrated by a DTGS TEC detector. In the photocurrent measurements, the indium contacts were fabricated on both sides of the *n-p* junction samples and on the side of thin film on glass substrate sample C. The structure of the studied sample has been characterized by x-ray diffraction (XRD) and Raman measurements, which were performed on a Bruker-axs D8 Advance instrument in the standard θ-2θ configuration and a Jobin Yvon LabRAM HR 800UV micro-Raman system in backscattering configuration (with a laser wavelength 514.5 nm), respectively.

Figure 1 presents the photocurrent (a) and Raman spectra (b) of the studied nc-Si:H thin films and the reference samples of *a*-Si:H (extremely low crystal fraction) and c-Si

a)Author to whom correspondence should be addressed. Electronic mail: rongzhang@dbc.shmtu.edu.cn.
b)Electronic mail: wzshen@sjtu.edu.cn.

TABLE I. Sample structure, growth method and conditions (temperature, power density, and pressure), thin film thickness, as well as crystalline fraction X_C. Fano resonance parameters obtained by fitting first-order Raman spectra of the nc-Si:H thin films at room temperature with the Fano line shape of Eq. (1).

Samples	Method	Temperature (°C)	Power density (W/cm^2)	Pressure (Torr)	Thickness (μm)	X_c (%)	Γ (cm^{-1})	$\Delta\omega$ (cm^{-1})	q
A:c-Si(n)/c-Si(p)	Czochralski	~1400	···	···	···	>99	···	···	···
B:nc-Si:H(n)/c-Si(p)	PECVD	250	0.5	1.0	0.9	57	9.5	3.5	−4.5
C: nc-Si:H(n)/glass	PECVD	250	0.4	1.0	1.0	46	12	−0.5	−3.9
D:nc-Si:H(n)/c-Si(p^+)	PECVD	250	0.3	0.4	1.4	6	34	−23.8	−3.4
E:a-Si:H(n)/c-Si(p^+)	PECVD	250	0.02	0.2	1.3	<1	···	···	···

(extremely high crystal fraction), where solid curves are the experimental results and scatters are the asymmetric line shapes of the phonon due to the Fano interference. In Fig. 1(a), the photocurrent peak with the photon energy of 1.2 eV becomes more and more obvious, as demonstrated by the more and more steep on the photon energy edge of 1.05 eV (bulk Si band gap) in the photocurrent spectra of these studied samples from E to A. For the a-Si thin film sample E, it shows a wide photocurrent peak with photon energy of 1.8 eV, as universally reported for the a-Si:H thin film.[7] For the c-Si sample A, it shows a typical broad photocurrent peak with photon energy beyond 1.05 eV and a small drop in the high-absorption region. While in the other three nc-Si:H thin film samples, a gradual feature of double peak is clearly observed on the photocurrent spectra within the photon energy regime between 1.05 and 1.8 eV. Moreover, the double-peak photocurrent becomes sharper and sharper from sample D to B. It is obvious that the variation of photocurrent spectra is mainly caused by the change of electronic states in these samples due to the different microstructures, which are determined by the growth conditions, such as grow temperature and power. Table I lists the corresponding detailed sample growth information of these studied samples.

We start with the structural information for exploring the microstructure variation in the above studied samples through the Raman experiments. Figure 1(b) presents the Raman spectra by the solid curves for all the studied samples, including both the c-Si sample A and a-Si thin film sample E as references. The Raman spectra clearly exhibit the typical transverse optical structure of a symmetric peak at 521.3 cm^{-1} (as marked by dotted line) in the c-Si sample A[8] and an asymmetric peak at 480 cm^{-1} in the a-Si:H thin film sample E.[9] In the other three nc-Si:H thin films (samples B, C, and D), the Raman spectra show the asymmetric peaks with the peak positions varying from ~520 to ~480 cm^{-1} involving the contributions from both ordered structure of the Si nanocrystals at ~520 cm^{-1} and the disordered structure of the a-Si:H boundaries at ~480 cm^{-1}. Due to the different atomic vibration modes in the disordered and ordered structure, the asymmetric Raman peak is the reflection of both the amorphous and crystalline contributions in the studied nc-Si:H thin film samples.[10] The crystalline fraction (X_C) was obtained by the ratio of the integrated intensity of the crystalline contributions to the total integrated intensity of the Raman transverse optical peak, and listed in Table I.

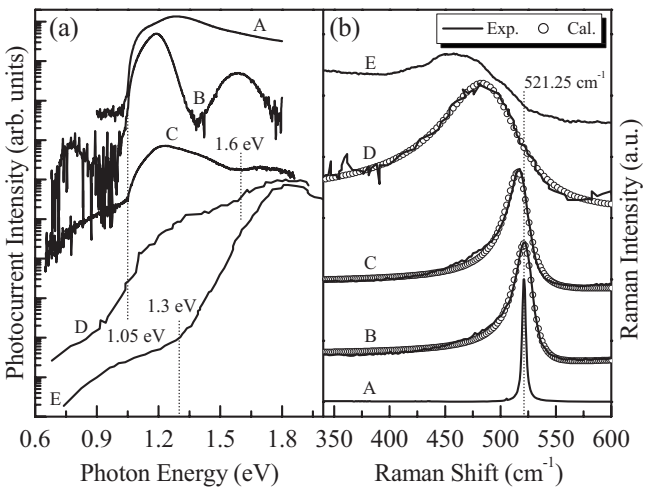

FIG. 1. (a) Experimental photocurrent and (b) Raman (solid curves) spectra, as well as the calculation of the Fano curves (scatters) for the nc-Si:H thin film samples (B, C, and D). Detailed sample information of crystalline fraction X_C and extracted Fano resonance parameters have been listed in Table I.

In combination with the Raman spectra and the photocurrent spectra in Fig. 1, we can draw the conclusion that the photocurrent peak with the photon energy above 1.3 eV is mainly contributed from the disordered structure as demonstrated by the Raman peak of ~480 cm^{-1} in the a-Si:H thin film sample E, and the photocurrent peak at the photon energy of 1.05 eV is mainly contributed from the ordered structure as demonstrated by the Raman peak of ~520 cm^{-1} in the c-Si sample A. While the double-peak photocurrent with the photon energy ranging from 1.05 to 1.8 eV was caused by the ordered and disorder structure in the studied nc-Si:H samples. Moreover, the photocurrent edge at the photon energy of 1.05 eV becomes more and more distinguishable with the increasing crystal fraction. The steep photocurrent edge at 1.05 eV indicates the band gap transitions in the continuous energy band of bulk Si, as demonstrated in the reference c-Si sample A. Therefore, a Si-like continuous energy band with the extended state is gradually developed with increasing structural order and crystalline fraction. This will be further demonstrated by the below XRD results.

Figure 2 presents the experimental XRD results by solid curves for the nc-Si:H thin film samples of B and C, as well as that of the c-Si sample A as a reference. The XRD spectra of the three samples all display the peaks with the typical Si material feature caused by the ordered structure of Si atomic lattice, i.e., two clear diffraction peaks of (111) and (220), together with a dim (331) peak. In the nc-Si:H thin film samples, the diffraction peaks become much wider with decreasing crystalline fraction. The larger broadening of the diffraction peak reflects the smaller grain size in the studied sample, as revealed by the Scherrer formula.[11] The average grain sizes are obtained by Lorentzian fitting (circle scatters), 6.9 nm for sample B and 2.9 nm for sample C. In addition, an appreciable low-angle ($2\theta < 15°$) XRD scattering is in-

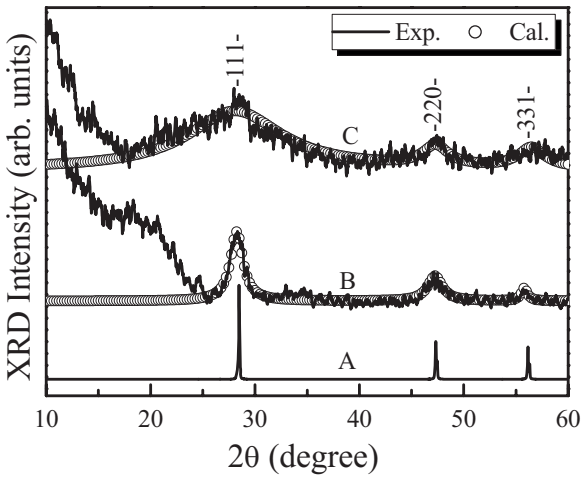

FIG. 2. Experimental XRD spectra (solid curves) and theoretical results (scatters) of the nc-Si:H samples (B and C), as well as the c-Si sample A as a reference.

dicative of the actual nanometer-size voids within the nc-Si:H thin films.[12] In the *a*-Si thin film, the low-angle XRD scattering becomes the main feature, and the above three typical XRD peaks would becomes more and more wide and even unobservable due to the low grain density and grains size in the level of 1–2 nm.[13] Therefore, the XRD results clearly demonstrate the nanometer Si crystals with the ordered structure of Si atomic lattice in the nc-Si:H thin film, where the crystal fraction becomes smaller with the grain size decreasing.

The nc-Si:H thin film sample consists of nc-Si crystals separated by *a*-Si:H boundaries or voids, as revealed by the structure information from the above Raman and XRD experimental results. It is the low dimensional structure of the separated nc-Si crystals by grain boundaries that results in the discrete states in the nc-Si:H thin film.[14] Furthermore, the extended state can also be formed in the nc-Si:H thin film when the crystal fraction is high enough and the grain boundary is narrow enough, comparable to the electronic wavelength of ~10 nm at room temperature. Therefore, both the discrete state and extended state can be existed in the nc-Si:H thin films at the same time, where an interference between the discrete and extended states can take place. This is the Fano interference,[15] where the asymmetric line shapes of the phonon as described in Ref. 16 is expressed as

$$I(\varepsilon,q)=\frac{(q+\varepsilon)^2}{1+\varepsilon^2} \quad \text{and} \quad \varepsilon=\frac{\omega-\omega_0-\triangle\omega_0}{\Gamma}, \tag{1}$$

where ω_0 and $\omega_0+\Delta\omega_0$ are the phonon frequencies in pure Si and in the nc-Si:H thin films, respectively. Γ and q are broadening and asymmetry parameters. $\Delta\omega_0$, Γ, and q mainly depend on the phonon self-energy and the electron-phonon interaction. The Fano resonance shapes with different Γ and q are clearly observed in the nc-Si:H thin films with different crystalline fractions, as shown by the well agreement between the experimental results of solid curves and the calculated results (circle scatters) in Fig. 1(b). By fitting the Raman spectra with Eq. (1), the above three parameters of $\Delta\omega_0$, Γ, and q are extracted and listed in Table I, where the broadening Γ decreases and asymmetry q increases with the increase of crystalline fraction. This phenomenon is also demonstrated by the variation of Fano resonance shapes with increasing structural order through decreasing doping density.[8,16] In the lowly doped or pure c-Si sample with nearly perfect ordered structure, the Fano resonance disappears due to the disappearance of the discrete state.

It is the extended state due to highly ordered structure that significantly improves the carrier transport in the nc-Si:H thin film sample, leading to the high photogenerated carriers collection efficiency. While the discrete state due to the disorder structure of grain boundary or voids is disadvantages to the free carriers transport, it destroys the crystal moment and symmetry selection rules in phonon aiding subband-gap transition due to the loss of translational symmetry at the grain boundaries. The discrete state can result in the directive transitions within the nc-Si:H thin film.[5] Therefore, the high density nanometer-size voids enlarges the surface-to-volume ratio in the nc-Si:H thin film, i.e., improve the optical absorption cross section. The directive transition plays an important role for the enhancement of optical absorption, resulting in the above phenomena of high photocurrent response.

In summary, the high density of nanometer embedded in the very thin *a*-Si:H boundaries results in a superposition of a Si-like continuous energy band in the tail band of *a*-Si:H in the nc-Si:H thin film. This is clearly demonstrated by the double-peak photocurrent with photon energy above 1.05 eV and at 1.6 eV (respectively close to the band gap of c-Si and *a*-Si:H), further by the double-peak photocurrent varying with the crystalline fraction, and also by the Fano interference due to the interaction between extended state and discrete state. Therefore, the double role of grain boundary can allow us to achieve very high photocurrent response, even beyond that of c-Si,[5] in the nc-Si:H thin film.

This work was supported by the Natural Science Foundation of China under Contract No. 10674094, the Shanghai Municipal Key Project No. 08XD14022, the Innovation Program of Shanghai Municipal Education Commission under Contract Nos. 09YZ238 and 2007CG43, and the Expenditure Budget Program of Shanghai Municipal Education Commission under Contract No. 2008074.

[1] O. Morton, Nature (London) **443**, 19 (2006).
[2] R. W. Collins, A. S. Ferlauto, G. M. Ferreira, C. Chen, J. Koh, R. J. Koval, Y. H. Lee, J. M. Pearce, and C. R. Wronski, Sol. Energy Mater. Sol. Cells **143**, 78 (2003).
[3] X. Y. Chen, W. Z. Shen, and Y. L. He, J. Appl. Phys. **97**, 024305 (2005).
[4] R. S. Crandall, J. Appl. Phys. **53**, 3350 (1982).
[5] R. Zhang, X. Y. Chen, K. Zhang, and W. Z. Shen, J. Appl. Phys. **100**, 104310 (2006).
[6] R. Zhang, X. Y. Chen, J. J. Lu, and W. Z. Shen, J. Appl. Phys. **102**, 123708 (2007).
[7] A. V. Gelatos, K. K. Mahavadi, J. D. Cohen, and J. P. Harbison, Appl. Phys. Lett. **53**, 403 (1988).
[8] M. Chandrasekhar, J. B. Renucci, and M. Cardona, Phys. Rev. B **17**, 1623 (1978).
[9] M. H. Brodsky, M. Cardona, and J. J. Cuomo, Phys. Rev. B **16**, 3556 (1977).
[10] I. Kaiser, N. H. Nickel, W. Fuhs, and W. Pilz, Phys. Rev. B **58**, R1718 (1998).
[11] M. R. Fitzsimmons, J. A. Eastman, M. Müller-Stach, and G. Wallner, Phys. Rev. B **44**, 2452 (1991).
[12] S. C. Moss and J. F. Graczyk, Phys. Rev. Lett. **23**, 1167 (1969).
[13] S. Vepřek, F.-A. Sarott, and Z. Iqbal, Phys. Rev. B **36**, 3344 (1987).
[14] X. Y. Chen and W. Z. Shen, Appl. Phys. Lett. **85**, 287 (2004).
[15] U. Fano, Phys. Rev. **124**, 1866 (1961).
[16] F. Cerdeira, T. A. Fjeldly, and M. Cardons, Phys. Rev. B **8**, 4734 (1973).